3-2008

ARABIDOPSIS TRITHORAX1 Dynamically Regulates FLOWERING LOCUS C Activation via Histone 3 Lysine 4 Trimethylation

Stephane Pien
University of Zurich, pien@botinst.uzh.ch

Delphine Fleury
Ghent University/Vlaams Instituut voor Biotechnologie

Joshua S. Mylne
John Innes Centre

Pedro Crevillen
John Innes Centre

Dirk Inze
Ghent University/Vlaams Instituut voor Biotechnologie

See next page for additional authors

The Plant Cell, Vol. 20: 580–588, March 2008, www.plantcell.org © 2008 American Society of Plant Biologists

ARABIDOPSIS TRITHORAX1 Dynamically Regulates *FLOWERING LOCUS C* Activation via Histone 3 Lysine 4 Trimethylation [W]

Stéphane Pien,[a,b,c,1] Delphine Fleury,[c] Joshua S. Mylne,[d] Pedro Crevillen,[d] Dirk Inzé,[c] Zoya Avramova,[e] Caroline Dean,[d] and Ueli Grossniklaus[a]

[a] Institute of Plant Biology, Zürich-Basel Plant Science Center, University of Zürich, Zurich CH-8008, Switzerland
[b] Institut für Pflanzenwissenschaften, Zürich-Basel Plant Science Centre, Eidgenössische Technische Hochschule-Zentrum, Zurich CH-8092, Switzerland
[c] Department of Plant Systems Biology, Ghent University/Vlaams Instituut voor Biotechnologie, B-9052, Belgium
[d] Department of Cell and Development Biology, John Innes Centre, Norwich NR4 7UH, United Kingdom
[e] School of Biological Sciences, University of Nebraska, Lincoln, Nebraska 68588-0118

***Trithorax* function is essential for epigenetic maintenance of gene expression in animals, but little is known about *trithorax* homologs in plants. ARABIDOPSIS TRITHORAX1 (ATX1) was shown to be required for the expression of homeotic genes involved in flower organogenesis. Here, we report a novel function of ATX1, namely, the epigenetic regulation of the floral repressor *FLOWERING LOCUS C* (*FLC*). Downregulation of *FLC* accelerates the transition from vegetative to reproductive development in *Arabidopsis thaliana*. In the *atx1* mutant, *FLC* levels are reduced and the *FLC* chromatin is depleted of trimethylated, but not dimethylated, histone 3 lysine 4, suggesting a specific trimethylation function of ATX1. In addition, we found that ATX1 directly binds the active *FLC* locus before flowering and that this interaction is released upon the transition to flowering. This dynamic process stands in contrast with the stable maintenance of homeotic gene expression mediated by *trithorax* group proteins in animals but resembles the dynamics of plant *Polycomb* group function.**

INTRODUCTION

Epigenetic mechanisms play crucial roles in shaping and maintaining cell identity and in patterning the body plan during development. Epigenetic information is partly carried by histone proteins in the form of reversible covalent modifications at their N-terminal tails. In *Drosophila melanogaster*, the *Polycomb* group (PcG) and *trithorax* group (trxG) proteins form higher-order complexes, which antagonistically repress and maintain the expression of homeotic genes (*HOX* genes), respectively (Simon and Tamkun, 2002). PcG and trxG complexes contain SET (for Suppressor of variegation 3-9, Enhancer of zeste, TRX) domain proteins that have histone methyltransferase (HMT) activity. They posttranslationally modify lysines on histones H3 and H4 (Lachner et al., 2004), thereby regulating the accessibility of the transcription machinery to the *HOX* gene clusters. These Lys methylation states have been classified as repressive and activating marks, depending on their effect on gene expression.

In recent years, several *Arabidopsis thaliana* PcG complexes were shown to repress their target genes via deposition of H3K27me3 marks (reviewed in Pien and Grossniklaus, 2007). This supports a conservation of the PcG function between plants and animals. Consequently, if *trithorax* functions were also conserved during evolution, trxG proteins may antagonistically regulate PcG target genes. Consistently, two *Arabidopsis* PcG target genes, the flowering time regulator *FLOWERING LOCUS C* (*FLC*) and the floral homeotic gene *AGAMOUS* (*AG*), show an enrichment of H3K4me2 and H3K4me3 marks at their chromatin, which correlates with active transcription (Bastow et al., 2004; He et al., 2004; Schubert et al., 2006). In *Drosophila*, such marks are deposited by the trxG protein Trithorax (TRX) and in mouse by the mixed-lineage leukemia (MLL) protein. The presence of H3K4me marks suggests that *trithorax* homologs and their associated functions exist in *Arabidopsis*.

Five close homologs of TRX and MLL were identified in the *Arabidopsis* genome and named *ARABIDOPSIS TRITHORAX* (*ATX1-5*) (Alvarez-Venegas and Avramova, 2001; Baumbusch et al., 2001). ATX1 is predicted to contain a SET domain (Alvarez-Venegas et al., 2003) that has both histone binding and HMT activity (Rea et al., 2000; Katsani et al., 2001). In vitro assays demonstrated that H3K4 is a substrate for ATX1's HMT activity, while mutant isoforms of ATX1 lacking part of the SET domain have no activity (Alvarez-Venegas et al., 2003). Loss of *ATX1* leads to flower homeotic defects and affects leaf morphogenesis (Alvarez-Venegas et al., 2003). Recently, ATX1 was shown to bind *AG* chromatin and to be required for H3K4me3 deposition at this locus (Saleh et al., 2007).

Transcriptional profiling in the *atx1* mutant allowed us to identify *FLC*, a flowering time regulator, as a putative ATX1

[1] Address correspondence to pien@botinst.uzh.ch.
The author responsible for distribution of materials integral to the findings presented in this article in accordance with the policy described in the Instructions for Authors (www.plantcell.org) is: Ueli Grossniklaus (grossnik@botinst.uzh.ch).
[W] Online version contains Web-only data.
www.plantcell.org/cgi/doi/10.1105/tpc.108.058172

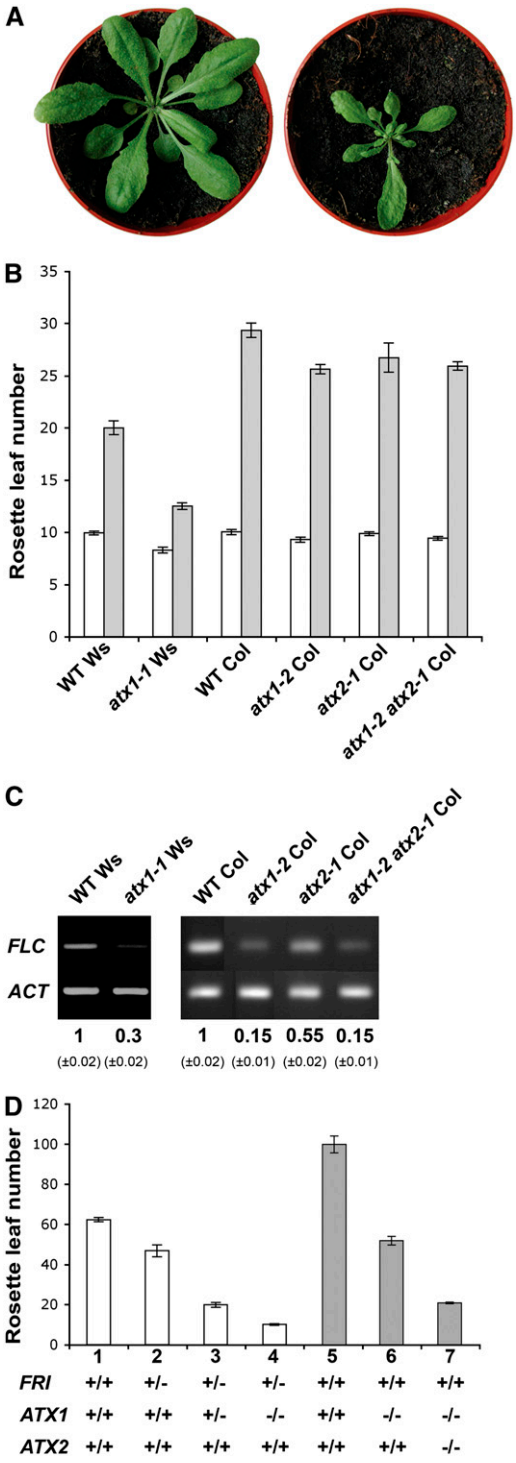

Figure 1. Characterization of *atx* Mutants.

(A) At flowering, the *atx1* (Ws) rosette lf (**[A]**, right) is smaller than the wild type (**[A]**, left), with a reduction in the leaf number in *atx1* compared with the wild type.

(B) The average number of rosette leaves at flowering, a measure of flowering time, is reduced in *atx1* and *atx2* mutants. Open bars, leaf number at flowering under long-day conditions; gray bars, short-day conditions. All data are presented as means ± SE ($n = 15$ to 20; $P < 0.05$ using Student's *t* test).

(C) RT-PCR quantification of *FLC* transcripts in the wild type and in *atx1* and *atx2* mutants. Left panel, wild type (Ws) and *atx1-1* (Ws) mutant; right panel, wild type (Col), *atx1-2* (Col), and *atx2-1* (Col) mutants. Numbers (±SE) refer to *FLC* transcript level relative to the wild type of three independent biological replicate experiments. *ACT*, actin loading control.

(D) Average number of rosette leaves at flowering. *atx1-1* (Ws) mutants were crossed with Col plants (Col^{Sf-2}), into which the wild-type San Feliu-2 (Sf-2) flowering-time locus *FRIGIDA* (FRI^{Sf-2}) had been introgressed (Lee and Amasino, 1995) (white columns). *atx1-2 atx2-1* (Col) double mutants were crossed with Col^{Sf-2} (gray columns). Columns 1 to 4 represent segregating F2 populations; the origin of the relevant alleles is indicated. Columns 5 to 7 are from a homogeneous background resulting from crosses between Col^{Sf-2} and Col. 1, FRI^{Sf-2} (Col^{Sf-2}) *ATX1* (Col^{Sf-2}) ($n = 12$); 2, FRI^{Sf-2}/*fri* (Col^{Sf-2}/Ws) *ATX1* (Col^{Sf-2}) ($n = 46$); 3, FRI^{Sf-2}/*fri* (Col^{Sf-2}/Ws) *ATX1*/*atx1* (Col^{Sf-2}/Ws) ($n = 67$); 4, FRI^{Sf-2}/*fri* (Col^{Sf-2}/Ws) *atx1-1* (Ws) ($n = 38$); 5, FRI^{Sf-2} (Col^{Sf-2}) *ATX1* (Col) *ATX2* (Col); 6, FRI^{Sf-2} (Col^{Sf-2}) *atx1-2* (Col) *ATX2* (Col); 7, FRI^{Sf-2} (Col^{Sf-2}) *atx1-2* (Col) *atx2-1* (Col). In a heterozygous FRI^{Sf-2}/*fri* background, the introduction of one *atx1* copy results in a reduced number of leaves at flowering time. The suppression of *FRI* had a greater effect on flowering time in the *atx1* (Ws) background. In a Col^{Sf-2} background carrying the FRI^{Sf-2} allele, the *atx1-1 atx2-1* double mutant suppressed the late-flowering phenotype more dramatically than the *atx1-2* single mutant. All data are presented as means ± SE ($n = 12$ to 67; $P < 0.05$ using Student's *t* test).

target gene. *FLC* encodes a MADS domain transcription factor that functions as a repressor of the floral transition. Transcriptional regulation of *FLC* has been well studied and shown to be associated with chromatin modifications, but little was known about the activation and maintenance of expression of this central gene. Therefore, we studied *FLC* regulation as a model to decipher the molecular mechanism of *trithorax* function in plants and to gain insight into novel functions of the *ATX1* gene. We showed that both single and double mutation of *ATX1* and its closest homolog *ATX2* (Alvarez-Venegas and Avramova, 2001) lead to early flowering, correlating with a reduction of *FLC* transcripts levels. *ATX1* and its target gene *FLC* are coexpressed in a spatio-temporal manner. Using chromatin immunoprecipitation (ChIP), we showed that ATX1 binds at the *FLC* locus and its presence correlates with H3K4me3 modifications. Furthermore, ChIP analyses revealed that ATX1 not only activates *FLC* but it also prevents its repression, since H3K27me2 repressive marks are deposited in the absence of ATX1 function. Finally, our study identified ATX1 as a direct transcriptional activator of *FLC*.

RESULTS

atx1 and *atx2* Are Early-Flowering Mutants Affecting the *FLC* Expression Level

The *atx1-1* mutation was previously reported to delay the transition to flowering (Alvarez-Venegas et al., 2003). These studies, however, did not quantify the changes in flowering time or leaf number at bolting. Therefore, we investigated the *atx1-1* mutant in more detail to decipher how the flowering transition was affected. In contrast with previously published work (Alvarez-Venegas et al., 2003), under our growth conditions *atx1*mutations

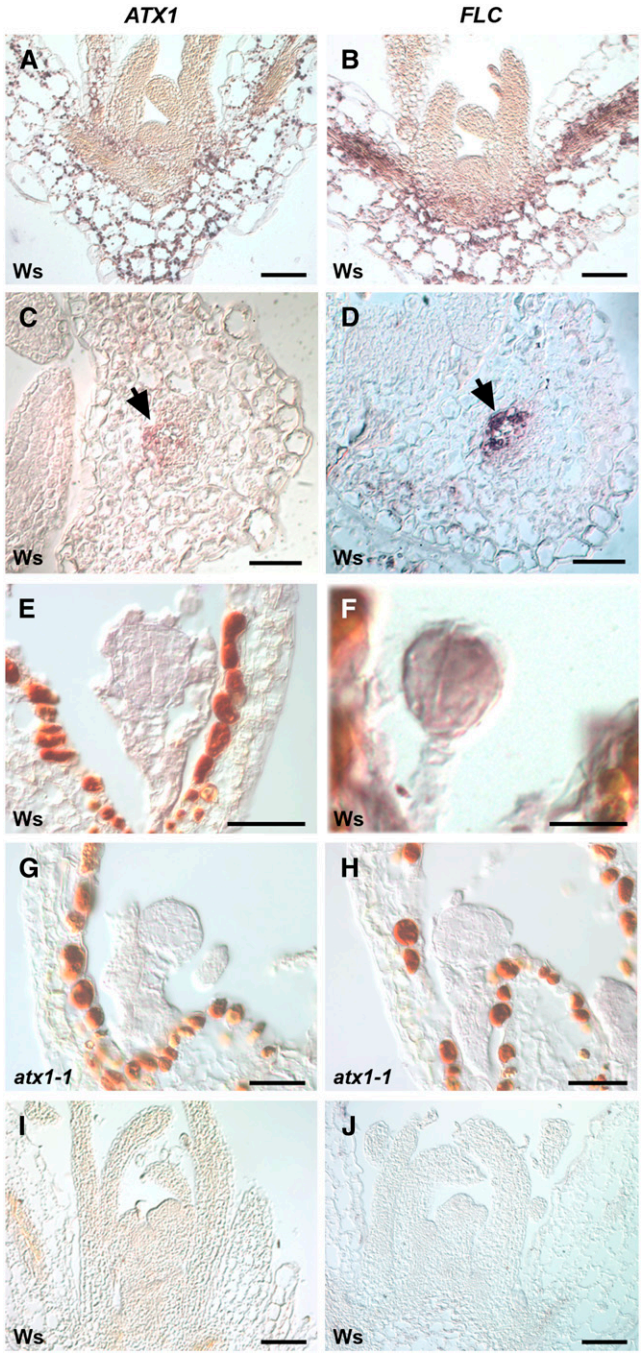

Figure 2. Spatio-Temporal Expression Patterns of *ATX1* and *FLC* in Wild-Type and *atx1-1* Tissue as Assayed by in Situ Hybridization.

(A), **(C)**, **(E)**, **(G)**, and **(I)** Sections probed with an antisense *ATX1* probe.
(B), **(D)**, **(F)**, **(H)**, and **(J)** Sections probed with an antisense *FLC* probe. Wild-type tissue sections hybridized with sense probes for *ATX1* and *FLC* gave no signal at any developmental stage.
(A) and **(B)** Ten-day-old seedlings with *ATX1* and *FLC* transcripts accumulating in the vasculature and the hypocotyl.
(C) and **(D)** Ten-day-old seedlings. Cross sections of the first pair of leaves, with *ATX1* and *FLC* transcripts accumulating in the vasculature (arrows).
(E) and **(F)** Wild-type globular embryos showing expression of both *ATX1* and *FLC*.
(G) and **(H)** In *atx1-1* globular embryos, neither *ATX1* nor *FLC* transcripts are detectable.
(I) and **(J)** At flowering, neither *ATX1* nor *FLC* message is detectable in the wild-type vasculature.

led to an early-flowering phenotype in the rapid-flowering accessions Wassilewskija (Ws) and Columbia (Col), as measured by the number of rosette leaves at bolting (Figures 1A and 1B). *atx1-1* mutants flowered early under both long-day and short-day conditions, showing that *ATX1* is involved in repressing the transition to flowering, independently of the photoperiod.

To investigate the molecular basis of the early-flowering phenotype of *atx1-1* mutant plants, we performed RNA profiling experiments with 10-d-old *atx1-1* and wild-type seedlings using the Affymetrix ATH1 GeneChip. To reveal whether trxG and PcG proteins play similar antagonistic roles as they do in animals (Simon and Tamkun, 2002), we looked for differentially expressed genes that had already been classified as PcG target genes. With these criteria, we found that the floral regulator *FLC*, a PcG target gene, had greatly reduced steady state transcript levels in the *atx1-1* mutant (3.4-fold decrease; see Supplemental Table 1 and Supplemental Table 2 online). This reduction was confirmed by RT-PCR in both *atx1-1* and *atx1-2* (Col) homozygous mutants (Figure 1C).

We further investigated the impact of *atx1* mutations on flowering time by crossing *atx1-1* and *atx1-2* mutants with a line containing an active *FRIGIDA* (*FRI*) allele (Lee and Amasino, 1995). The presence of the active *FRI* allele is associated with *Arabidopsis* late-flowering accessions and results in a high level of *FLC* expression. Loss of *ATX1* strongly suppressed the late-flowering effect of *FRI* in a dosage-dependent manner (Figure 1D). Thus, *ATX1* is required for the increased expression of *FLC* that results from overexpression of *FRI* in the line containing an active *FRI* allele.

Mutation of the closest homolog of *ATX1*, *ATX2* (Alvarez-Venegas and Avramova, 2001), revealed a role for *ATX2* in *FLC* regulation (Figure 1C). In a *FRI* background, the *atx1-2 atx2-1* double mutant suppressed the late-flowering phenotype more dramatically than in the *atx1-2* single mutant (Figure 1D), suggesting that *ATX1* and *ATX2* play a partially redundant role in activating *FLC*.

ATX1 and *FLC* Are Spatio-Temporally Coexpressed

Since we found that *ATX1* and *ATX2* regulate *FLC*, we analyzed the spatio-temporal expression of these three genes by in situ hybridization. If *ATX1* and *ATX2* directly regulate *FLC* during the plant life cycle, then the spatio-temporal expression patterns of *ATX1*, *ATX2*, and *FLC* are expected to overlap. In situ hybridization analyses for *ATX1* and *FLC* in 10-d-old seedlings revealed expression of both genes in the vasculature of the cotyledons, hypocotyls, and the first pair of leaves (Figures 2A to 2D). The pattern of *FLC* mRNA accumulation reproduces the expression pattern of the reporter gene *uidA*, encoding β-*glucuronidase* (*GUS*), translationally fused to *FLC* (*FLC-GUS*) (Bastow et al., 2004). Both *ATX1* and *FLC* transcripts were present in overlapping

patterns during embryogenesis (Figures 2E and 2F). *FLC* transcript was not detected in *atx1-1* embryos, suggesting that *ATX1* is necessary to activate *FLC* well before the floral induction pathways are active (Figures 2G and 2H). Just prior to flowering, a strong reduction of both *ATX1* and *FLC* transcript levels occurred in the vasculature of wild-type plants (Figures 2I and 2J). The overlap of the spatio-temporal expression patterns of the two genes is consistent with a direct regulation of *FLC* by *ATX1*. These data were confirmed by a cross between a *FRI* line containing an *FLC-LUCIFERASE* (*FLC-LUC*) translational fusion (Mylne et al., 2004) and the *atx1-2* mutation (Figures 3A and 3B). In *FRI FLC-LUC* plants, *FLC* was highly expressed, as indicated by the *FLC-LUC* signal in the vasculature and the shoot apex (Figure 3A). In *FRI FLC-LUC atx1-2* lines, *FLC* expression was strongly reduced in the vasculature (Figure 3B). Interestingly, *ATX1* expression could not be detected in the shoot apical meristem of wild-type plants (Figure 2A), and mutations in *ATX1* did not lead to a loss of *FLC* expression in that tissue (Figure 3B), suggesting that *FLC* expression in the shoot apical meristem is positively regulated by some other factor(s). We investigated the expression pattern of *ATX2* at the same developmental stage. *ATX2* was expressed in the vasculature and, unlike *ATX1*, was also detected in the shoot apical meristem (see Supplemental Figure 1 online). In *FRI FLC-LUC atx1-2 atx2-1* lines, *FLC* expression was strongly reduced in the vasculature and in the shoot apex (Figure 3C). However, *FLC* expression was still detectable in the shoot apical meristem of *FRI FLC-LUC atx1-2 atx2-1* lines, confirming that *ATX1* and *ATX2* play their major role in the vasculature.

ATX1 Is Required for the Deposition of H3K4me3 Marks at the *FLC* Locus

To address whether ATX1-dependent histone modifications are involved in the regulation of *FLC*, we analyzed chromatin modifications at the *FLC* locus by ChIP at three regions surrounding the translational start codon (Figure 4A). These regions are essential for *FLC* transcription and function (Bastow et al., 2004; Kim et al., 2005), and H3K4me3 marks in these regions correlate with *FLC* transcription (He et al., 2004). We found that H3K4me3 levels were reduced in region B and undetectable in region A in *atx1-1* mutants (Figure 4B) compared with wild-type plants at the same developmental stage. Just prior to floral induction, H3K4me3 levels decreased in wild-type plants to levels similar to those in *atx1-1* mutant seedlings. Taken together, these findings suggest that *ATX1* is required for the establishment of the H3K4me3 mark at the *FLC* locus to promote and/or maintain a transcriptionally active state.

In plants and animals, H3K4 can be either, mono-, di-, or trimethylated. These three epigenetic marks can be interpreted differently by the transcription machinery depending on the organism (Fuchs et al., 2006). Therefore, we quantified in parallel H3K4me2 and H3K4me3 marks at the *FLC* locus in wild-type and *atx1-1* plants. Surprisingly, region B, which covers the transcription start site of *FLC*, displayed elevated levels of H3K4me2 in 10-d-old *atx1-1* seedlings compared with the wild type (Figure 4B). In regions A and C, this mark was almost at the same level as in wild-type plants. At later developmental stages, prior to the flowering transition, a similar pattern could be observed. Altogether, the loss of *ATX1* activity strongly impaired the deposition of H3K4me3 marks but did not suppress the deposition of H3K4me2 marks at *FLC* chromatin. These findings suggest that the function of *ATX1* seems to be specific for the deposition of the H3K4me3 mark.

Loss of H3K4me3 marks at the *FLC* locus induces a gain of H3K27me2 marks

Since in the *atx1-1* mutant, *FLC* is depleted in the H3K4me3 activation mark and is transcriptionally repressed, we measured the levels of H3K27me2 and H3K27me3, two marks previously shown to correlate with *FLC* repression (Bastow et al., 2004; Sung et al., 2006). In the regions A and B, an increased level of H3K27me2 was observed in *atx1-1* mutant seedlings compared with wild-type seedlings at the same stage. H3K27me2 levels also increased, although less dramatically, prior to flowering. In wild-type plants, the level of H3K4me3 inversely correlated with the level of H3K27me2. However, H3K27me2 marks were still present on *FLC* chromatin in regions A and B during active

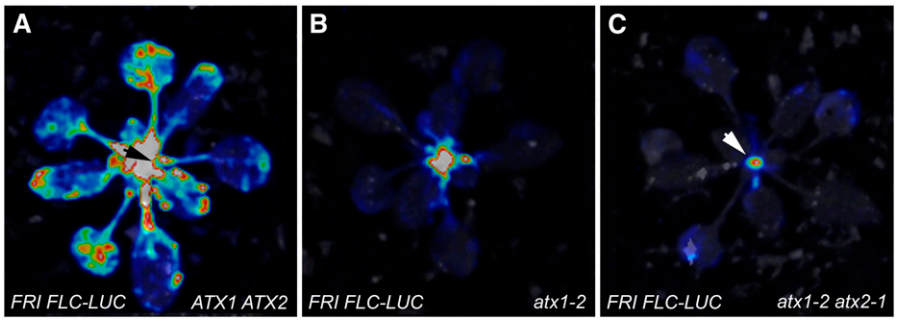

Figure 3. *FLC-LUC* Expression Pattern in *FRI*, *FRI atx1-2*, and *FRI atx1-2 atx2-1* Plants.

(A) In *FRI FLC-LUC* lines, *FLC* is highly expressed in the vasculature and the shoot apex (arrow).
(B) In *FRI FLC-LUC atx1-2* lines, *FLC* expression is strongly reduced in the vasculature.
(C) In *FRI FLC-LUC atx1-2 atx2-1* lines, *FLC* expression is strongly reduced in the vasculature and in the shoot apex (arrow).
Twenty-five-day-old plants were analyzed for *FLC-LUC* expression for all lines analyzed. Two biological replicates were performed, growing side by side 10 plants of each genotype.

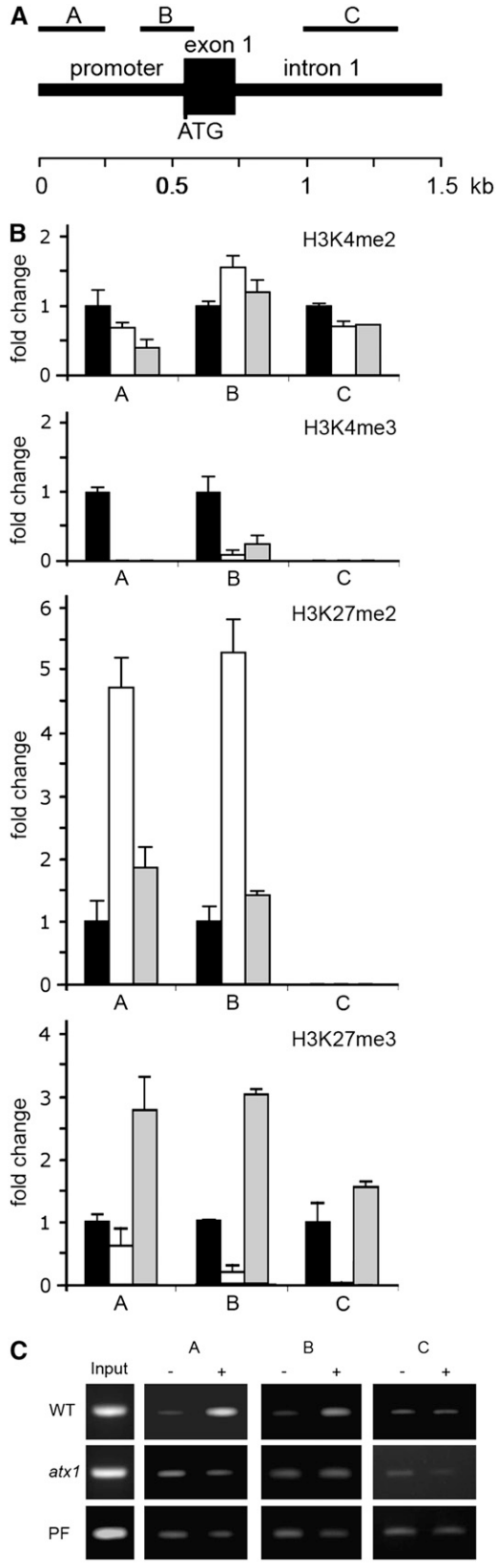

Figure 4. Histone Modifications and ATX1 Binding at the *FLC* Locus.

(A) Genomic structure of the *FLC* promoter and regions investigated by ChIP. The thick lines represent the 5′ untranslated region and intron 1, while the black box represents the translated region of exon 1. Regions amplified by PCR are labeled A to C.

(B) Relative levels of histone modifications in *FLC* chromatin were analyzed by PCR from at least three replicate ChIP assays using H3K4me2-, H3K4me3-, H3K27me2-, and H3K27me3-specific antibodies. Black bars, 10-d-old Ws seedlings; open bars, 10-d-old *atx1-1* mutant seedlings; gray bars, 16-d-old wild-type plants prior to flowering. Means are calculated based on at least three independent experiments and are given with bars indicating 1 SE.

(C) ChIP assay using an ATX1-specific antibody. Regions A, B, and C were examined for ATX1 enrichment in *FLC* chromatin. +, ATX1 antibody; −, no antibody controls. Regions A and B showed enrichment of ATX1 in Ws seedlings. PF, 16-d-old Ws plants prior to flowering.

transcription of the gene prior to the flowering transition. Similarly, low H3K27me3 levels could be detected in wild-type seedlings at the *FLC* chromatin in all regions investigated (Figure 4B). It is worth noting that the presence of this repressive mark together with the activating mark H3K4me3 does not prevent active transcription of *FLC*. The level of the H3K27me3 mark, however, substantially increased in plants prior to flowering, which correlates with *FLC* repression at that developmental stage. This is consistent with the observation that H3K27me3 deposition by plant PcG proteins correlates with transcriptional repression of the *Arabidopsis* PcG target genes *MEDEA* (*MEA*), *PHERES1* (*PHE1*), *AG*, *SHOOTMERISTEMLESS* (*STM*), and *AGAMOUS-LIKE 19* (*AGL19*) (Gehring et al., 2006; Jullien et al., 2006; Makarevich et al., 2006; Schönrock et al., 2006; Schubert et al., 2006).

ATX1 Directly Interacts with *FLC* Chromatin to Regulate Its Transcription

The ability of *ATX1* to promote H3K4me3 deposition suggests that ATX1 directly interacts with the *FLC* locus to modify its chromatin state via its HMT activity (Alvarez-Venegas et al., 2003). We investigated this possibility by ChIP (Figure 4C) using an antibody raised against ATX1. We found that ATX1 was enriched at the *FLC* chromatin (regions A and B) in wild-type seedlings relative to *atx1-1* mutants. In the wild type, ATX1 was not enriched in region C, which is consistent with the absence of the H3K4me3 mark in that region (Figure 4B). These data show that ATX1 binding to the *FLC* chromatin correlates with the deposition of H3K4me3 marks. In wild-type plants at the floral transition, when *FLC* is downregulated, ATX1 binding at the *FLC* locus could not be detected. This observation suggests that ATX1 dynamically binds the *FLC* locus to regulate its transcription.

DISCUSSION

The trxG Genes *ATX1* and *ATX2* Are Required to Activate *FLC* Expression

Our study provides strong evidence that *ATX1*, a homolog of the *Drosophila trx* protein, is required to control flowering transition and acts to upregulate *FLC* expression. *ATX1* acts downstream of, or in parallel with, *FRI* in an interdependent manner. It also

acts directly on *FLC* and binds to its promoter and transcription start site regions. Many regulators of *FLC* transcription have been described (reviewed in He and Amasino, 2005), but, unlike ATX1, these do not appear to modify *FLC* chromatin directly. The putative HMT *EARLY FLOWERING IN SHORT DAYS* (*EFS*), a homolog of the trxG *Drosophila* protein Absent small homeotic disks1 (ASH1) (Tripoulas et al., 1994), was shown to be necessary for the deposition of H3K4me3 marks at *FLC* chromatin of winter annual accessions (He et al., 2004). In such accessions, vernalization (extended exposure to cold) is required to activate the VRN *Polycomb* Repressive Complex 2 (VRN-PRC2) (Levy et al., 2002; Kim et al., 2005), which represses *FLC*, leading to flowering. However, in the commonly studied rapid-flowering accession Col, vernalization is not required for flowering, and mutations in *EFS* do not affect the level of H3K4me3 at the *FLC* locus (He et al., 2004). In this context, our data provide evidence that ATX1 regulates *FLC* transcription in the rapid-flowering accessions Ws and Col. Additionally, in lines containing an active *FRI* allele, which mimic winter annual accessions, the *atx1-1 atx2-1* double mutant suppressed the late-flowering phenotype, suggesting that genes of the *ATX* family are also central for *FLC*-mediated regulation in winter annual accessions. How *ATX1*, *ATX2*, and *EFS* collaborate in this process remains unclear and would require additional investigations. Our data suggest that *ATX1* and *ATX2* are involved in the same pathway since the early-flowering phenotype observed in single mutants is not more severe in the *atx1-2 atx2-1* double mutant. However, in the *FRI* background, mutation of both genes leads to a shorter vegetative phase compared with *atx1* single mutants in the same background. This may be explained by delayed transcription of *ATX2*, whose expression is detected later than *ATX1* during the vegetative phase and which may have a stronger impact in winter annual accessions than in rapid-flowering accessions.

PcG and trxG Proteins Dynamically Regulate *FLC* Expression

In contrast with animals, where PcG and trxG proteins play a role in the permanent repression or activation of genes whose expression state was determined by other factors, in plants, PcG and trxG proteins dynamically interact in the regulation of target genes, such as *FLC*, during the plant life cycle (reviewed in Pien and Grossniklaus, 2007). In wild-type plants at the floral transition, when *FLC* transcripts are no longer detectable in the apex and neighboring vasculature, ATX1 binding at the *FLC* locus could not be detected (Figure 4C). This indicates that ATX1 dynamically binds the *FLC* locus to regulate its transcription. In *Drosophila*, TRX together with members of the PRC1/2 complexes are constitutively bound to the HOX *Ultrabithorax* (*Ubx*) locus independent of whether the *Ubx* gene is actively transcribed or not (Papp and Müller, 2006). In contrast with the situation in *Drosophila* and mammals, ATX1 binding is not stable,

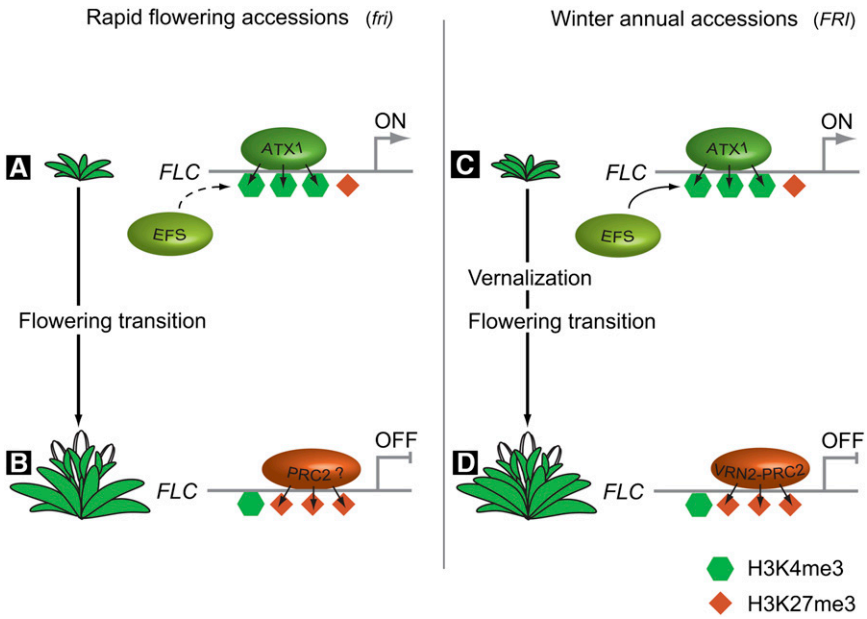

Figure 5. Model for Dosage-Dependent Regulation of *FLC* Expression by Chromatin Modifications.

(A) In rapid-flowering accessions (*fri* background), *FLC* is activated by ATX1 via the deposition of H3K4me3 marks at the *FLC* 5′ untranslated region during the vegetative phase.

(B) The H3K27me3 repressive mark is present but does not prevent *FLC* expression. EFS is required to prevent early flowering but does not modify the level of H3K4me3 marks at the *FLC* locus (Kim et al., 2005). The removal of H3K4me3, together with an increased level of H3K27me3 mark deposited by a still unknown PRC2 complex, leads to *FLC* repression and subsequent flowering.

(C) In winter annual accessions (*FRI* background), ATX1 together with EFS activates *FLC* expression via the deposition of H3K4me3 marks.

(D) A prolonged cold treatment (vernalization) induces the VRN2-PRC2 complex, which in turn represses *FLC* via the deposition of H3K27me3 marks.

which points to a dynamic function of trxG complexes in plants. This dynamic process is reflected by the removal of previously deposited H3K4me3 at the *FLC* promoter during the transition from vegetative to reproductive development (Figure 4B). Recently, dynamic regulation was also demonstrated for PcG proteins (Baroux et al., 2006). Together, these data suggest that plant PcG and trxG proteins affect a wide range of gene expression programs and potentially contribute to plant developmental plasticity.

FLC Is Regulated through Dosage-Dependent Interactions of Activating and Repressive Histone Modifications

The results presented here highlight the importance of the H3K4me3 modification mediated by ATX1 for the transcriptional activation of *FLC*: the levels of H3K4me2 in the *atx1* mutants are clearly not sufficient in this context. However, we cannot rule out that the deposition of H3K4me2 marks does not play a role in active *FLC* transcription. A recent study provided evidence on the requirement of *FCA* together with *FLOWERING LOCUS D* (*FLD*) to mediate H3K4 demethylation of *FLC* in its central region and, thus, to silence the gene (Liu et al., 2007). By contrast, at several *Arabidopsis* loci, the H3K4me2 mark was shown to be associated with the H3K27me2 mark, independent of whether the associated genes were actively transcribed or not (Alvarez-Venegas and Avramova, 2005).

Surprisingly, our data showed that repressive H3K27me2 and H3K27me3 modifications were present at the *FLC* locus during active transcription and *FLC* silencing. This observation is in agreement with the whole-genome analysis of H3K27me3 distribution in the *Arabidopsis* Ws accession, where this mark was detected at *FLC* chromatin during active transcription (Zhang et al., 2007). However, it is notable that the levels of H3K27me2 and H3K27me3 marks at *FLC* are always lower than the levels observed in plants prior to flowering, where *FLC* is silenced (Figure 4B). The presence of repressive marks at the *FLC* locus during its active expression can be interpreted as basal levels that are not sufficient to repress *FLC* expression in that context. Therefore, our results suggest a mechanism where the active or repressive state of *FLC* expression depends on the accumulation of repressive and activating marks in a dosage-dependent manner (i.e., the expression of *FLC* correlates with the deposition of H3K4me3 marks and basal levels of H3K27me2 and H3K27me3 marks at the *FLC* promoter). Conversely, repression of *FLC* is associated with the removal of H3K4me3 marks and a substantial increase of H3K27me3 marks at the *FLC* promoter (see model in Figure 5).

The absence of H3K4me3 marks at *FLC* chromatin in the *atx1-1* mutant is correlated with an accumulation of H3K27me2 (Figure 4B), a mark associated with *FLC* gene repression (Bastow et al., 2004). This suggests the presence of a default mechanism that represses *FLC* transcription in the absence of H3K4me3 marks. A similar mechanism was described in *Drosophila*, where the trxG proteins ASH1 and TRX have been proposed to counteract PcG repression, either by histone binding and/or H3K4-trimethylation, which subsequently prevents the binding of PcG proteins to *HOX* genes (Klymenko and Müller, 2004). The simultaneous binding of TRX and PcG proteins at the *Ubx* locus challenged this hypothesis (Papp and Müller, 2006). Recently, ASH1 binding at the *Ubx* locus was shown to correlate with H3K4me3 deposition and to occur only when *Ubx* is transcribed (Papp and Müller, 2006). Therefore, ASH1 was proposed to counteract PcG repression via the deposition of the H3K4me3 marks, which subsequently restricts H3K27 methylation in the promoter and coding regions. Whether or not this mechanism is conserved in plants will require more investigations; however, our study provides evidence for a similar mechanism in *Arabidopsis* using different histone marks.

In the *atx1-1* mutant background, the accumulation of H3K27me3 marks was reduced in the promoter and the first intron, arguing for the requirement of ATX1 and/or the presence of H3K4me3 marks for the deposition of this repressive mark. A similar result was recently observed at the *AG* locus, where ATX1 is required for the trimethylation of H3K27 in the promoter and the downstream coding region (Saleh et al., 2007). By contrast, the *atx1-1* mutation results in an increased level of another repressive mark at *FLC*, H3K27me2, showing that ATX1 activity is not required for the deposition of this repressive mark. This suggests that in the absence of the H3K4me3 mark in this region, the H3K27me3 mark is not required to repress *FLC*.

In summary, we demonstrate that ATX1 directly regulates the floral regulator *FLC* by mediating the H3K4me3 modification. Additionally, we show that H3K4me3 deposition is accompanied by a decrease in H3K27me2 levels at the *FLC* locus. Thus, we propose that the developmentally regulated binding of ATX1 and trimethylation of H3K4 at *FLC* chromatin counteract *FLC* silencing. Our study also shows that transition to flowering correlates with the release of ATX1 from the *FLC* locus and an increase of the level of H3K27me3 repressive marks, of which a critical level is required to achieve full repression of *FLC* (Shindo et al., 2006). This time- and dosage-dependent regulation resembles the vernalization process, where prolonged exposure to cold leads to progressive silencing of *FLC* (Chouard, 1960; Lang, 1965). Chromatin-mediated regulation of *FLC*, and probably other genes, is not an all-or-nothing process and fine-tuning may be achieved through different levels of histone modifications.

METHODS

Plant Material and Growth Conditions

Seeds, wild-type Ws, and *atx1-1* (Ws) (Alvarez-Venegas et al., 2003), wild-type Col, *atx1-2* (Col) (SALK_149002), *atx2-1* (Col) (SALK_074806), and *FRI* (Col^{Sf-2}) plants, in which the flowering-time locus *FRI* has been introgressed from the Sf-2 accession into a Col background (Lee and Amasino, 1995), were grown on Murashige and Skoog media with 15 g/L of sucrose at 4°C for 2 d under short-day conditions (8/16 h day/night) with 10 μmol photons m^{-2} s^{-1} white light and then transferred to 20°C under either long-day (16/8 h day/night) or short-day conditions with 57 μmol photons m^{-2} s^{-1} white light. Luciferase imaging was as described by Mylne et al. (2004), and the images were obtained using a NightOwl imaging system (Berthold Technologies).

atx1-1 plants were genotyped using SP26 (forward) 5′-TCTATGCAGCTCTTTGCTAATTGG-3′ and TDNA-LB SP11 (reverse) 5′-GATGCACTCGAAATCAGCCAATTTTAGAC-3′ or SP26 (forward) and SP27 (reverse) 5′-AGCCCAGAGCATGAGCTTACC-3′ for the wild-type *ATX1* gene. *atx1-2* plants were genotyped using JM341 (forward) 5′-GGTATAGCTCATGCTCTGGGC-3′ and SALK-LB (reverse) 5′-CCAAACTGGAACAACACTCAAC-3′ or JM341 (forward) and JM340 (reverse) 5′-TCTCTTTTGTGGACTTGCTGTG-3′ for the wild-type *ATX1* gene. *atx2-1*

plants were genotyped using JM345 (forward) 5′-GCTGCAAAGAA-CAAACTCTTCC-3′ and SALK-LB (reverse) or JM345 (forward) and JM346 (reverse) 5′-AGGCCACCAATAGCTGACAAG-3′ for the wild-type *ATX2* gene.

RT-PCR Analyses

RT-PCR quantifications were performed with 10-d-old seedlings. RNA was isolated with the Trizol reagent (Invitrogen) according to the manufacturer's instructions. RT-PCR for *FLC* was performed using *FLC*-specific primers SP135 (forward) 5′-TTGGATCAGTCAAAAGC-3′ and SP136 (reverse) 5′-AGTAGTGGGAGAGTCACGGG-3′, and *ACTIN2* (*ACT2*) control primers were SP105 (forward) 5′-GCCCTCGTTTGT-GGGAATGG-3′ and SP106 (reverse) 5′-AAGCCTTTGATCTTGAGAGC-3′. Signal intensities using ethidium bromide staining (0.4 μg/mL) were normalized relative to *ACTIN2* PCR products with ImageQuant software (Molecular Dynamics). These results are representative of three independent biological replicate experiments. Fold changes are the mean of three independent quantifications from three independent RNA extractions. Primer efficiency was tested to quantify *FLC* and *ACT2* PCR product in the logarithmic phase.

In Situ Hybridization

Fixation and hybridization were performed as previously described (Köhler et al., 2003). Primers used to make the probes were as follows: *ATX1*, SPG63 (forward) 5′-AGCTGGATCCAGTCTGATGTCTAAGAAGG-3′ and SPG64 (reverse) 5′-ACGTGAATTCCCTTACACCTTCTTAAACC-3′; *ATX2*, SPG54 (forward) 5′-ATGCGGATCCGGAAGATCAGTCCTCGTAC-3′ and SPG55 (reverse) 5′-AGCTGAATTCTTTCTGAAGTTGATCCATC-3′; *FLC*, SPB1 (forward) 5′-AGCTGGATCCTTGGATCATCAGTCAAAAGC-3′ and SPB2 (reverse) 5′-AGCTGAATTCAGTAGTGG GAGAGTCACCGG-3′.

ChIP

ChIP was performed on 10-d-old seedlings and 16-d-old plants prior to flowering, grown under long-day conditions, as previously described (Köhler et al., 2003). Antibodies used were H3K4me2 (Upstate), H3K4me3 (Upstate), H3K27me2 (Upstate), H3K27me3 (Upstate), and ATX1 (GenScript). Primers for *ACTIN2/7* and for *FLC* regions A (Bastow et al., 2004), B (He et al., 2004), and C (Bastow et al., 2004) were as previously described. PCR conditions were similar to the ones used by Bastow et al. (2004) and He et al. (2004), where analysis to show the amplification efficiency of all primer pairs used in the chromatin immunoprecipitation analysis has been published. Signal intensities using ethidium bromide staining (0.4 μg/mL) were normalized relative to *ACTIN* 2/7 PCR products with ImageQuant software (Molecular Dynamics), and the fold changes are expressed relative to the value of wild-type seedlings. Means are given with bars indicating 1 SE.

Accession Numbers

Sequence data from this article can be found in the Arabidopsis Genome Initiative database under the following accession numbers: AG, At4g18960; AGL19, At4g22950; ATX1, At2g31650; ATX2, At1g05830; EFS, At1g77300; FCA, At4g16280; FLD, At3g10390; FLC, At5g10140; FRI, At4g00650; MEA, At1g02580; PHE1, At1g65330; STM, At1g62360.

Supplemental Data

The following materials are available in the online version of this article.

Supplemental Figure 1. Spatio-Temporal Expression Patterns of *ATX2* in Wild-Type 10-d-Old Seedlings Assayed by in Situ Hybridization.

Supplemental Table 1. Steady State Message Levels in the *atx1-1* Homozygous Mutant Compared with Wild-Type Ws.

Supplemental Table 2. Downregulated Genes in the *atx1-1* Homozygous Mutant Compared with Wild-Type Ws.

Supplemental References.

ACKNOWLEDGMENTS

S.P. thanks Nikolaus Amrhein (Eidgenössische Technische Hochschule) for his support and continuous interest in this project. We thank three anonymous reviewers for helpful suggestions, Sharon Kessler, Célia Baroux, Stephen Schauer, and Mark Curtis (all at the University of Zurich, Switzerland) for comments on the manuscript, and the ABRC for provision of the SALK T-DNA lines. This work was supported by an EMBO long-term fellowship to S.P., the University of Zurich, the Eidgenössische Technische Hochschule, and grants from the Swiss National Science Foundation and the European Union's FP6 Network of Excellence ''The Epigenome'' to U.G.

Received January 17, 2008; revised March 4, 2008; accepted March 10, 2008; published March 28, 2008.

REFERENCES

Alvarez-Venegas, R., and Avramova, Z. (2001). Two *Arabidopsis* homologs of the animal *trithorax* genes: A new structural domain is a signature feature of the *trithorax* gene family. Gene **271:** 215–221.

Alvarez-Venegas, R., and Avramova, Z. (2005). Methylation patterns of histone H3 Lys 4, Lys 9 and Lys 27 in transcriptionally active and inactive *Arabidopsis* genes and in *atx1* mutants. Nucleic Acids Res. **33:** 5199–5207.

Alvarez-Venegas, R., Pien, S., Sadder, M., Witmer, X., Grossniklaus, U., and Avramova, Z. (2003). *ATX1*, an *Arabidopsis* homolog of *trithorax*, activates flower homeotic genes. Curr. Biol. **13:** 627–637.

Baroux, C., Gagliardini, V., Page, D.R., and Grossniklaus, U. (2006). Dynamic regulatory interactions of *Polycomb* group genes: *MEDEA* autoregulation is required for imprinted gene expression in *Arabidopsis.* Genes Dev. **20:** 1081–1086.

Bastow, R., Mylne, J.S., Lister, C., Lippman, Z., Martienssen, R.A., and Dean, C. (2004). Vernalization requires epigenetic silencing of *FLC* by histone methylation. Nature **427:** 164–167.

Baumbusch, L.O., Thorstensen, T., Krauss, V., Fischer, A., Naumann, K., Assalkhou, R., Schulz, I., Reuter, G., and Aalen, R.B. (2001). The *Arabidopsis thaliana* genome contains at least 29 active genes encoding SET domain proteins that can be assigned to four evolutionarily conserved classes. Nucleic Acids Res. **29:** 4319–4333.

Chouard, P. (1960). Vernalization and its relations to dormancy. Annu. Rev. Plant Physiol. **11:** 191–237.

Fuchs, J., Demidov, D., Houben, A., and Schubert, I. (2006). Chromosomal histone modification patterns – From conservation to diversity. Trends Plant Sci. **11:** 199–208.

Gehring, M., Huh, J.H., Hsieh, T.F., Penterman, J., Choi, Y., Harada, J.J., Goldberg, R.B., and Fischer, R.L. (2006). DEMETER DNA glycosylase establishes *MEDEA Polycomb* gene self-imprinting by allele-specific demethylation. Cell **124:** 495–506.

He, Y., Doyle, M.R., and Amasino, R.M. (2004). PAF1-complex-mediated histone methylation of *FLOWERING LOCUS C* chromatin is required for the vernalization-responsive, winter-annual habit in *Arabidopsis.* Genes Dev. **18:** 2774–2784.

He, Y., and Amasino, R.M. (2005). Role of chromatin modification in flowering-time control. Trends Plant Sci. **10:** 30–35.

Jullien, P.E., Katz, A., Oliva, M., Ohad, N., and Berger, F. (2006). *Polycomb* group complexes self-regulate imprinting of the *Polycomb* group gene *MEDEA* in *Arabidopsis.* Curr. Biol. **16:** 486–492.

Katsani, K.R., Arredondo, J.J., Kal, A.J., and Verrijzer, C.P. (2001). A homeotic mutation in the *trithorax* SET domain impedes histone binding. Genes Dev. **15:** 2197–2202.

Kim, S.Y., He, Y., Jacob, Y., Noh, Y.S., Michaels, S., and Amasino, R. (2005). Establishment of the vernalization-responsive, winter-annual habit in *Arabidopsis* requires a putative histone H3 methyltransferase. Plant Cell **17:** 3301–3310.

Klymenko, T., and Müller, J. (2004). The histone methyltransferases Trithorax and Ash1 prevent transcriptional silencing by *Polycomb* group proteins. EMBO Rep. **5:** 373–377.

Köhler, C., Hennig, L., Spillane, C., Pien, S., Gruissem, W., and Grossniklaus, U. (2003). The *Polycomb*-group protein MEDEA regulates seed development by controlling expression of the MADS-box gene *PHERES1.* Genes Dev. **17:** 1540–1553.

Lachner, M., Sengupta, R., Schotta, G., and Jenuwein, T. (2004). Trilogies of histone lysine methylation as epigenetic landmarks of the eukaryotic genome. Cold Spring Harb. Symp. Quant. Biol. **69:** 209–218.

Lang, A. (1965). Physiology of flower initiation. In Encyclopedia of Plant Physiology, Vol. 15, W. Ruhland, ed (Berlin: Springer-Verlag), pp. 1380–1536.

Lee, I., and Amasino, R. (1995). Effect of vernalization, photoperiod, and light quality on the flowering phenotype of *Arabidopsis* plants containing *FRIGIDA* gene. Plant Physiol. **108:** 157–162.

Levy, Y.Y., Mesnage, S., Mylne, J.S., Gendall, A.R., and Dean, C. (2002). Multiple roles of *Arabidopsis VRN1* in vernalization and flowering time control. Science **297:** 243–246.

Liu, F., Quesada, V., Crevillén, P., Bäurle, I., Swiezewski, S., and Dean, C. (2007). The *Arabidopsis* RNA-binding protein FCA requires a lysine-specific demethylase 1 homolog to downregulate *FLC.* Mol. Cell **28:** 398–407.

Makarevich, G., Leroy, O., Akinci, U., Schubert, D., Clarenz, O., Goodrich, J., Grossniklaus, U., and Köhler, C. (2006). Different *Polycomb* group complexes regulate common target genes in *Arabidopsis.* EMBO Rep. **7:** 947–952.

Mylne, J., Greb, T., Lister, C., and Dean, C. (2004). Epigenetic regulation in the control of flowering. In Epigenetics, Vol. LXIX, B. Stillman and D. Stewart, eds (Cold Spring Harbor, NY: Cold Spring Harbor Laboratory Press), pp. 457–464.

Papp, B., and Müller, J. (2006). Histone trimethylation and the maintenance of transcriptional ON and OFF states by trxG and PcG proteins. Genes Dev. **20:** 2041–2054.

Pien, S., and Grossniklaus, U. (2007). *Polycomb* group and *trithorax* group proteins in *Arabidopsis.* Biochim Biophys Acta. **1769:** 375–382.

Rea, S., Eisenhaber, F., O'Carroll, D., Strahl, B.D., Sun, Z.W., Schmid, M., Opravil, S., Mechtler, K., Ponting, C.P., Allis, C.D., and Jenuwein, T. (2000). Regulation of chromatin structure by site-specific histone H3 methyltransferases. Nature **406:** 593–599.

Saleh, A., Al-Abdallat, A., Ndamukong, I., Alvarez-Venegas, R., and Avramova, Z. (2007). The *Arabidopsis* homologs of *trithorax* (ATX1) and *Enhancer of zeste* (CLF) establish 'bivalent chromatin marks' at the silent *AGAMOUS* locus. Nucleic Acids Res. **35:** 6290–6296.

Schönrock, N., Bouveret, R., Leroy, O., Borghi, L., Köhler, C., Gruissem, W., and Hennig, L. (2006). *Polycomb*-group proteins repress the floral activator *AGL19* in the *FLC*-dependent vernalization pathway. Genes Dev. **20:** 1667–1678.

Schubert, D., Primavesi, L., Bishopp, A., Roberts, G., Doonan, J., Jenuwein, T., and Goodrich, J. (2006). Silencing by plant *Polycomb*-group genes requires dispersed trimethylation of histone H3 at lysine 27. EMBO J. **25:** 4638–4649.

Shindo, C., Lister, C., Crevillen, P., Nordborg, M., and Dean, C. (2006). Variation in the epigenetic silencing of *FLC* contributes to natural variation in *Arabidopsis* vernalization response. Genes Dev. **20:** 3079–3083.

Simon, J.A., and Tamkun, J.W. (2002). Programming off and on states in chromatin: mechanisms of *Polycomb* and *trithorax* group complexes. Curr. Opin. Genet. Dev. **12:** 210–218.

Sung, S., Schmitz, R.J., and Amasino, R.M. (2006). A PHD finger protein involved in both the vernalization and photoperiod pathways in *Arabidopsis.* Genes Dev. **20:** 3244–3248.

Tripoulas, N.A., Hersperger, E., La Jeunesse, D., and Shearn, A. (1994). Molecular genetic analysis of the *Drosophila melanogaster* gene *absent, small or homeotic discs1* (*ash1*). Genetics **137:** 1027–1038.

Zhang, X., Clarenz, O., Cokus, S., Bernatavichute, Y.N., Pellegrini, M., Goodrich, J., and Jacobsen, S.E. (2007). Whole-genome analysis of histone H3 lysine 27 trimethylation in *Arabidopsis.* PLoS Biol. **5:** e129.

SUPPLEMENTAL Data

Supplemental Data. Pien et al. (2008). *ATX2* is expressed in the vasculature and the shoot apex meristem.

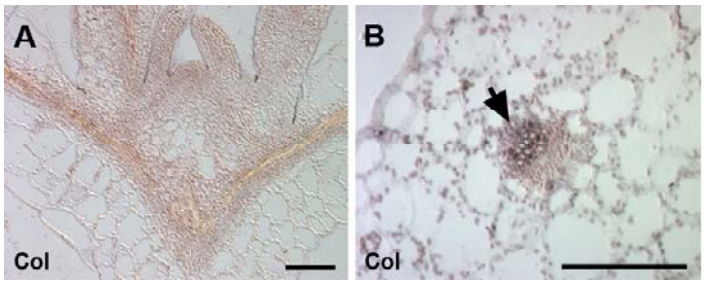

Supplemental Figure S1. Spatio-temporal expression patterns of *ATX2* in wild type 10-day-old seedlings assayed by *in situ* hybridization. A, B sections probed with anti-sense *ATX2*. A, *ATX2* transcripts accumulate in the vasculature of the leaves, the hypocotyls and in the shoot apex meristem. B, Leaf cross-sections with *ATX2* transcripts accumulating in the vasculature (black arrowhead). Wild type tissue sections hybridized with sense probes for *ATX2* gave no signal. Scale bars: 100 μm.

Supplemental Table 1. Steady state message levels of genes involved in flowering time regulation in *atx1-1* homozygous mutant compared to the wild type Ws.

			limma test	PA call		Pathway
gene	**At code**	**Fold change**	**p**	**Wt**	***atx1-1***	**/Function**
FT	At1g65480	0.89	1	A	A	Int
AP1	At1g69120	1.08	1	A	A	Int
MAF1	At1g77080	0.83	1	P	P	Rep
EFS	At1g77300	0.93	1	P	P	Rep
ELF7	At1g79730	1.14	1	P	P	Rep
ELF8	At2g06210	0.86	1	P	P	Rep
VEL3	At2g18870	0.93	1	A/P	M	Unknown
VEL2	At2g18880	1.02	1	A	A	Unknown
FVE	At2g19520	1.06	1	P	P	Auto
ATX1	At2g31650	0.28	1.24E-02	P	A	Rep
SOC1	At2g45660	0.79	1	P	P	Int
FLK	At3g04610	0.79	1	P	P	Auto
FLD	At3g10390	0.87	1	P	P	Auto
PIE1	At3g12810	1.15	1	P	P	Rep
VRN1	At3g18990	0.84	1	P	P	Vern
VRN5	At3g24440	1.03	1	P	P	Vern
SUF3	At3g33520	1.18	1	P	P	Rep
FRI	At4g00650	0.90	1	P	P	Rep
LD	At4g02560	1.06	1	P	P	Auto
FCA	At4g16280	1.05	1	P	P	Auto
VRN2	At4g16845	0.95	1	P	P	Vern
VIP3	At4g29830	1.19	1	P	P	Vern
VEL1	At4g30200	0.99	1	P	P	Unknown
FLC	At5g10140	0.29	9.92E-03	P	A	Rep
FY	At5g13480	1.05	1	P	P	Auto
CO	At5g15840	0.61	1	A/P	A/M	Int
FRL1	At5g16320	1.00	1	P	P	Rep
VIP4	At5g61150	1.12	1	P	P	Vern
LFY	At5g61850	1.07	1	A/P	A	Int
MAF2	At5g65050	0.86	1	P/M	P	Rep
MAF3	At5g65060	0.82	1	P/M	P/M/A	Rep
MAF4	At5g65070	0.95	1	A	A	Rep
MAF5	At5g65080	0.91	1	A	A	Rep

Table S1. Steady state message levels in *atx1-1* homozygous mutant compared to the wild type Ws.

RNA was extracted from the shoot apices of plants (comprising shoot apical meristem and first and second leaf primordia at the petiole-less stage) 10 days after germination using the Qiagen RNeasy kit (Qiagen GmbH, Hilden, Germany). This developmental stage is well before floral induction, such that *atx1-1* mutant seedlings are

indistinguishable from the wild type: therefore, only a minimal number of secondary transcriptional changes are expected. Microarray experiments were done by the VIB MicroArrays Facility lab (Leuven, Belgium; http://www.microarrays.be/) using ATH1 Affymetrix chips of 23,800 probes sets designed for *Arabidopsis* as described previously (Nelissen *et al*, 2005). Three replicates of each genotype were hybridized, with one replicate corresponding to one RNA extraction on an independent pool of plants. The raw data from Affymetrix GeneChip arrays (CEL files) was analyzed using GC Robust Multi-Array average method from *affy* and *rma* packages of Bioconductor Project Release 1.4 using R-1.9.0 software, and subsequently using a Bayesian t test of *limma* (Nelissen *et al*, 2005). The p values are calculated according to a Bayesian test of a linear model and corrected by Holm's method. The PA call corresponds to the transcript levels according to t test using MAS5.0 and comparing perfect match to mismatch probes for each probes set. A: no expression ($p>0.065$); M: medium expression ($0.065<p<0.05$); P: expressed gene ($p<0.05$). The reduction in steady state message levels for *FLC* was confirmed by quantitative RT-PCR (Figure 1C). The genes are classified into the following pathways or functions: Auto, autonomous pathway; Vern, vernalization pathway; Int, floral pathway integrators; Rep, Floral repressor.

Microarray data (accession number: E-MEXP-502) have been deposited at http://www.mged.org/Workgroups/MIAME/miame.html.

Supplemental Table S2. List of down-regulated genes in *atx1-1* homozygous mutant compared to the wild type Ws.

At code	Fold change	p	Gene Title
At3g28290	0.01	4.41E-09	integrin-related protein 14a
At1g58270	0.01	1.08E-08	meprin and TRAF homology domain-containing protein
At3g47250	0.02	8.77E-09	expressed protein
At1g31580	0.02	8.12E-09	expressed protein
At1g66100	0.03	4.41E-04	thionin, putative
At1g24793	0.03	8.61E-10	UDP-3-0-acyl N-acetylglucosamine deacetylase family protein
At1g73490	0.04	4.09E-08	RNA recognition motif (RRM)-containing protein
At4g15620	0.04	1.81E-07	integral membrane family protein
At3g46030	0.04	4.06E-06	histone H2B, putative
At1g35612	0.04	1.01E-07	expressed protein
At4g16890	0.05	5.00E-08	disease resistance protein (TIR-NBS-LRR class), putative
At1g23960	0.06	5.19E-06	expressed protein
At2g15050	0.06	1.31E-08	lipid transfer protein, putative
At3g16450	0.06	5.02E-05	jacalin lectin family protein
At5g10400	0.06	2.99E-08	histone H3
At4g16860	0.06	3.44E-07	disease resistance protein (TIR-NBS-LRR class), putative
At4g19500	0.06	3.78E-06	disease resistance protein (TIR-NBS-LRR class), putative
At4g16870	0.06	1.33E-05	copia-like retrotransposon family
At3g47220	0.06	5.05E-06	phosphoinositide-specific phospholipase C family protein
At1g03420	0.07	1.62E-06	expressed protein
At3g43740	0.07	2.67E-06	leucine-rich repeat family protein
At1g58842	0.07	5.23E-06	disease resistance protein (CC-NBS-LRR class), putative
At3g26290	0.07	6.65E-06	cytochrome P450 71B26, putative (CYP71B26)
At5g05060	0.08	7.40E-08	expressed protein
At1g59900	0.08	4.99E-04	pyruvate dehydrogenase E1 component alpha subunit, mitochondrial (PDHE1-A)
At1g73330	0.08	1.94E-03	protease inhibitor, putative (DR4)
At5g17880	0.08	3.28E-07	disease resistance protein (TIR-NBS-LRR class), putative
At1g63880	0.09	1.49E-05	disease resistance protein (TIR-NBS-LRR class), putative
At3g44630	0.09	8.76E-06	disease resistance protein RPP1-WsB-like (TIR-NBS-LRR class), putative
At4g16880	0.10	1.22E-04	disease resistance protein-related
At4g02540	0.10	9.59E-06	DC1 domain-containing protein
At5g41700	0.11	3.18E-07	ubiquitin-conjugating enzyme 8 (UBC8)
At1g11280	0.11	1.47E-06	S-locus protein kinase, putative
At3g27360	0.11	3.35E-06	histone H3
At4g12310	0.11	2.99E-04	cytochrome P450, putative
At5g40950	0.11	1.32E-06	50S ribosomal protein L27, chloroplast, putative (RPL27)
At4g13720	0.11	9.97E-05	inosine triphosphate pyrophosphatase, putative / HAM1 family protein
At4g20480	0.11	8.71E-08	expressed protein
At2g40010	0.12	3.41E-04	60S acidic ribosomal protein P0 (RPP0A)
At3g46530	0.12	7.77E-05	disease resistance protein, RPP13-like (CC-NBS class), putative
At1g56510	0.13	2.75E-06	disease resistance protein (TIR-NBS-LRR class), putative
At1g16260	0.13	2.37E-07	protein kinase family protein
At3g06160	0.13	1.65E-03	transcriptional factor B3 family protein
At1g24996	0.14	2.78E-03	expressed protein
At1g65370	0.15	2.51E-05	meprin and TRAF homology domain-containing protein
At5g56380	0.16	9.32E-06	F-box family protein
At2g03710	0.17	1.89E-04	MADS-box protein (AGL3)

At3g44890	0.17	8.60E-07	50S ribosomal protein L9, chloroplast (CL9)
At5g17890	0.17	2.10E-04	LIM domain-containing protein / disease resistance protein-related
At3g53650	0.17	3.98E-06	histone H2B, putative
At5g05750	0.17	5.44E-06	DNAJ heat shock N-terminal domain-containing protein
At3g14210	0.17	1.14E-03	myrosinase-associated protein, putative
At5g42250	0.18	8.69E-03	alcohol dehydrogenase, putative
At3g28270	0.20	1.56E-03	expressed protein
At4g36520	0.20	1.93E-06	trichohyalin-related
At4g19530	0.21	2.86E-03	disease resistance protein (TIR-NBS-LRR class), putative
At3g44610	0.21	1.46E-04	protein kinase family protein
At3g29120	0.21	3.06E-03	hAT-like transposase family (hobo/Ac/Tam3)
At1g23020	0.22	5.83E-04	ferric-chelate reductase, putative
At1g28670	0.22	2.60E-03	lipase, putative
At2g14880	0.22	3.62E-06	SWIB complex BAF60b domain-containing protein
At5g43580	0.23	2.50E-03	protease inhibitor, putative
At5g56910	0.24	1.01E-05	expressed protein
At5g51620	0.24	1.34E-03	expressed protein
At3g21950	0.25	1.16E-03	S-adenosyl-L-methionine:carboxyl methyltransferase family protein
At5g55790	0.25	3.96E-05	expressed protein
At3g01660	0.25	1.02E-02	expressed protein
At5g63020	0.25	1.36E-04	disease resistance protein (CC-NBS-LRR class), putative
At3g25760	0.25	4.02E-02	early-responsive to dehydration stress protein (ERD12)
At2g21860	0.25	3.51E-04	violaxanthin de-epoxidase-related
At5g46510	0.25	2.38E-03	disease resistance protein (TIR-NBS-LRR class), putative
At2g26470	0.26	3.20E-05	expressed protein
At1g52100	0.26	7.29E-04	jacalin lectin family protein
At2g44200	0.26	7.48E-03	expressed protein
At1g54260	0.26	5.13E-03	histone H1/H5 family protein
At3g28220	0.27	2.09E-02	meprin and TRAF homology domain-containing protein
At1g66970	0.27	4.26E-02	glycerophosphoryl diester phosphodiesterase family protein
At5g53150	0.27	2.11E-02	DNAJ heat shock N-terminal domain-containing protein
At5g44580	0.27	9.90E-03	expressed protein
At5g65390	0.27	1.36E-05	arabinogalactan-protein (AGP7)
At2g31630	0.28	1.24E-02	trithorax 1 (ATX-1) (TRX1)
At5g44410	0.28	1.45E-02	FAD-binding domain-containing protein
At2g29090	0.28	9.76E-03	cytochrome P450 family protein
At1g20390	0.28	2.90E-05	gypsy-like retrotransposon family
At3g10200	0.29	3.24E-04	dehydration-responsive protein-related
At1g59124	0.29	3.28E-04	disease resistance protein (CC-NBS-LRR class), putative
At5g10140	0.29	9.92E-03	MADS-box protein flowering locus F (FLF)
At5g36930	0.29	1.36E-02	disease resistance protein (TIR-NBS-LRR class), putative
At1g75960	0.29	2.37E-02	AMP-binding protein, putative
At1g79000	0.29	2.76E-03	p300/CBP acetyltransferase-related protein 2 (PCAT2)
At5g43270	0.30	2.34E-02	squamosa promoter-binding protein-like 2 (SPL2)
At4g08110	0.30	6.41E-03	CACTA-like transposase family (Ptta/En/Spm)
At3g46980	0.30	1.84E-04	transporter-related
At5g56030	0.30	1.93E-02	heat shock protein 81-2 (HSP81-2)
At5g26270	0.30	1.53E-03	expressed protein
At1g23950	0.31	3.39E-04	expressed protein
At3g27200	0.31	3.72E-02	plastocyanin-like domain-containing protein
At1g58150	0.31	1.51E-02	hypothetical protein
At4g13890	0.31	1.84E-02	glycine hydroxymethyltransferase, putative
At4g36140	0.32	8.33E-04	disease resistance protein (TIR-NBS-LRR class), putative
At5g22860	0.32	8.39E-04	serine carboxypeptidase S28 family protein

At3g14240	0.32	1.10E-02	subtilase family protein
At3g53380	0.32	4.83E-05	lectin protein kinase family protein
At5g24150	0.32	2.31E-02	squalene monooxygenase 1,1 / squalene epoxidase 1,1 (SQP1,1)
At1g12400	0.33	2.49E-03	expressed protein
At4g16710	0.34	1.85E-02	glycosyltransferase family protein 28
At3g24890	0.34	1.22E-02	synaptobrevin-related
At3g60290	0.35	1.27E-02	oxidoreductase, 2OG-Fe(II) oxygenase family protein
AtMg01090	0.35	2.76E-02	expressed mitochondrial protein (ORF262)
At4g02130	0.35	2.18E-02	glycosyl transferase family 8 protein
At4g35240	0.35	3.85E-02	expressed protein
At1g10150	0.36	2.34E-03	expressed protein
At2g36570	0.36	5.77E-03	leucine-rich repeat transmembrane protein kinase, putative
At1g49630	0.37	1.03E-03	peptidase M16 family protein / insulinase family protein
At3g47680	0.37	7.12E-03	expressed protein
At1g69523	0.37	1.09E-02	UbiE/COQ5 methyltransferase family protein
At1g69550	0.37	5.26E-03	disease resistance protein (TIR-NBS class), putative
At1g49650	0.38	1.69E-02	cell death associated protein-related
At2g18280	0.38	1.48E-02	tubby-like protein 2 (TULP2)
At5g41650	0.39	1.85E-02	lactoylglutathione lyase family protein / glyoxalase I family protein
At5g22510	0.40	7.32E-04	beta-fructofuranosidase, putative / invertase, putative
At1g07640	0.40	6.71E-03	Dof-type zinc finger domain-containing protein
At5g50530	0.40	1.11E-02	CBS domain-containing protein
At1g27540	0.40	3.68E-03	F-box family protein
At1g68400	0.41	6.97E-03	leucine-rich repeat transmembrane protein kinase, putative
At5g42090	0.41	2.80E-03	expressed protein
At3g45930	0.42	1.05E-02	histone H4
At5g16220	0.43	1.41E-02	octicosapeptide/Phox/Bem1p (PB1) domain-containing protein
At4g39710	0.43	2.23E-02	immunophilin, putative / FKBP-type peptidyl-prolyl cis-trans isomerase, putative
At1g21730	0.43	2.21E-03	kinesin-related protein (MKRP1)
At1g56720	0.43	2.40E-02	protein kinase family protein
At1g22400	0.43	7.40E-03	UDP-glucoronosyl/UDP-glucosyl transferase family protein
At5g27270	0.43	1.37E-02	pentatricopeptide (PPR) repeat-containing protein
At3g63330	0.44	6.66E-03	protein kinase family protein
At5g50580	0.44	4.52E-02	SUMO activating enzyme, putative
At4g31530	0.44	3.22E-03	expressed protein
At1g62810	0.44	1.73E-02	copper amine oxidase, putative
At3g49360	0.44	1.45E-02	glucosamine/galactosamine-6-phosphate isomerase family protein
At1g31600	0.45	1.08E-02	oxidoreductase, 2OG-Fe(II) oxygenase family protein
At1g80960	0.45	3.60E-02	F-box protein-related
At3g05140	0.45	9.89E-03	protein kinase family protein
At3g24515	0.45	1.06E-03	ubiquitin-conjugating enzyme, putative
At1g63420	0.45	1.58E-02	expressed protein
At2g11260	0.46	1.80E-02	Hypothetical protein, complete cds, clone: RAFL16-43-P18
At5g63760	0.46	3.17E-03	IBR domain-containing protein
At2g13970	0.46	1.35E-02	Mutator-like transposase family
At5g50550	0.46	3.61E-03	WD-40 repeat family protein / St12p protein, putative
At2g33220	0.47	7.04E-03	expressed protein
At5g03340	0.47	6.79E-04	cell division cycle protein 48, putative / CDC48, putative
At4g19510	0.48	4.98E-02	disease resistance protein (TIR-NBS-LRR class), putative
At5g49170	0.49	7.15E-03	expressed protein
At5g16250	0.49	3.75E-02	expressed protein
At3g61480	0.49	2.51E-02	expressed protein
At1g06180	0.50	1.29E-02	myb family transcription factor

Supplemental Table S2. Down-regulated genes in *atx1-1* mutant compared to the wild-type Ws.

Data obtained from the microarray ATH1 experiment with RNA from shoot apex tissues. RNA was extracted from the shoot apices of plants (comprising shoot apical meristem and first and second leaf primordia at the petiole-less stage) 10 days after germination using the Qiagen RNeasy kit (Qiagen GmbH, Hilden, Germany). Genes were selected at a Holm's $p < 0.05$ and a ratio of expression < 0.50.

References

Nelissen, H., Fleury, D., Bruno, L., Robles, P., De Veylder, L., Traas, J., Micol, J.L., Van Montagu, M., Inze, D., Van Lijsebettens, M. (2005). The *elongata* mutants identify a functional Elongator complex in plants with a role in cell proliferation during organ growth. Proc. Natl. Acad. Sci. USA. *102*, 7754-7759.